



Agenzia nazionale per le nuove tecnologie,  
l'energia e lo sviluppo economico sostenibile



MINISTERO DELLO SVILUPPO ECONOMICO



Ricerca di Sistema elettrico

# Double Stabilized Stainless Steels Procurement

*Carlo Cristalli*

Report RdS/PAR2013/035

Double Stabilized Stainless Steels Procurement

Carlo Cristalli - ENEA

Settembre 2014

Report Ricerca di Sistema Elettrico

Accordo di Programma Ministero dello Sviluppo Economico - ENEA

Piano Annuale di Realizzazione 2013

Area: Produzione di energia elettrica e protezione dell'ambiente

Progetto: Sviluppo competenze scientifiche nel campo della sicurezza nucleare e collaborazione ai programmi internazionali per il nucleare di IV Generazione

Obiettivo: Sviluppo competenze scientifiche nel campo della sicurezza nucleare

Responsabile del Progetto: Mariano Tarantino, ENEA

## Double Stabilized Stainless Steels Procurement

### Descrittori

Tipologia del documento: **Rapporto Tecnico**

Collocazione contrattuale: **Accordo di programma ENEA-MSE su sicurezza nucleare e reattori di IV generazione**

Argomenti trattati: **Caratterizzazione dei Materiali  
Generation IV Reactors  
Reattori nucleari veloci**

### Sommario


This document reports the considerations concerning irradiation behavior, creep resistance and corrosion properties which lead to the procurement of DS4 steel.

### Note

Copia n.

In carico a:

2			NOME			
			FIRMA			
1			NOME			
			FIRMA			
0	EMISSIONE	22/09/14	NOME	Carlo Cristalli	Mariano Tarantino	Mariano Tarantino
			FIRMA			
REV.	DESCRIZIONE	DATA	REDAZIONE	CONVALIDA	APPROVAZIONE	

 <b>Ricerca Sistema Elettrico</b>	<b>Sigla di identificazione</b>	<b>Rev.</b>	<b>Distrib.</b>	<b>Pag.</b>	<b>di</b>
	ADPFISS – LP2 – 067	0	L	2	17

## INDEX

1. INTRODUCTION .....	3
2. CREEP BEHAVIOUR .....	5
3. BEHAVIOUR UNDER IRRADIATION; THE RESULTS OF THE EXPERIENCE “SUPERNOVA” .....	8
4. PRELIMINARY RESULTS OF THE CORROSION TESTS PERFORMED AT ENEA BRASIMONE .....	9
5. Scope of the Supply .....	11
6. Technical Specification – DS4 Steel .....	12
Chemical Composition .....	12
Production.....	12
Characterization Tests .....	13
Documentation follow up.....	13
7. BIBLIOGRAPHY .....	13
ANNEX – 1 - Fabbricazione lingotto DS4 .....	14
ANNEX – 2 – Rapporto d’Analisi Lingotto .....	17

# 1. INTRODUCTION

At the beginning of the '80s, within an experimental program carried out at the Saclay Center, the under electrons irradiations (1 MeV HVEM) have shown the effectiveness of the simultaneous presence of Ti and Nb on the swelling resistance of 316 and 15 Cr-15 Ni matrix. This experimental evidence lead CEA and ENEA to start the production and the characterization of the first double stabilized steels (DS). This first generation was widely characterized showing the strong influence of some additional elements on the structural stability of an austenitic matrix. A good high temperature creep resistance for an austenitic steel is essentially due to microprecipitation of carbides (avg. dim 10 nm) which result finely dispersed on the dislocations network. This sort of "in-service" precipitation is highly effective as movement inhibitor for linear defects. Increasing the internal "back stress" it forbids the dislocations glide. The presence in solid solution of a sufficient content in carbon and in elements characterized by high attitude to carbides formation, is then highly desirable. If this requirement is satisfied, a solubilization annealing at 1100°C is enough to ensure the presence of carbides (TiC and NbC in the case of DS steels) during high temperature expositions. A new parameter has then been defined in order to manage the precipitation of carbides; the Stabilization Ratio R. R ratio has been calculated as

$$(1) R = \frac{[Ti] + [Nb] - [N]}{[C]}$$

In the first generation double stabilized steels a high percentage in primary precipitation (the one occurring during annealing treatment) had been noticed. As a consequence the "in-service" precipitation resulted reduced, sometimes absent. In the first generation double stabilized steels the annealing temperature used, 1125°C, didn't result sufficient to obtain a good solubilization of "free" Ti and Nb also because of the high stabilization ratio (3,18 for the 316DS and 2,04 for the 15-15DS). The precipitation of carbides doesn't only act on the creep resistance of the material; it also has positive effects on the stability under irradiation. In figure 1 a graphical investigation of the first 90's about the dependence of swelling attitude on the primary precipitation and on the stabilization ratio is reported.

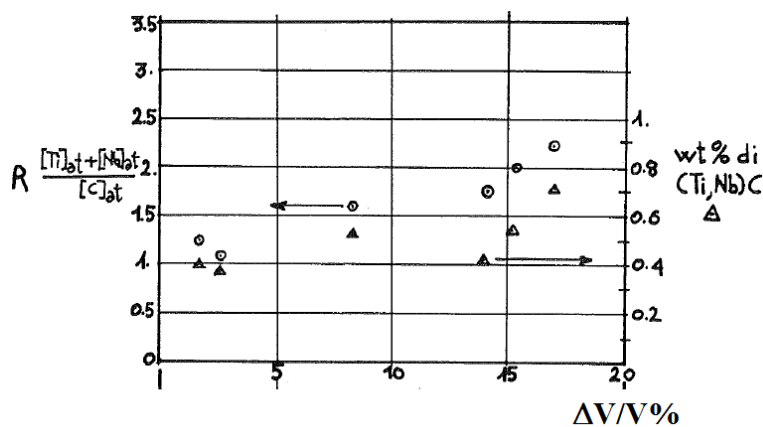


**Fig. 1. Relation between stabilization ratio, weight percentage of primary precipitation and swelling attitude for a 15Cr-15Ni austenitic matrix irradiated at 450°C with an irradiation damage of 105 dpa**

Regarding the previous Double Stabilization generation behaviour, the researchers have obtained a lower primary precipitation by modifications of chemical composition which lead to stabilization ratios of 1.38 for DS3 and 0.55 for the DS4 steel. With low stabilization ratios and a solution treatment at 1100°C it's possible to have a low primary precipitation, that means sufficient "free" contents of Carbon, Ti and Nb in solid solution in order to allow a secondary (in service) beneficial precipitation. A 2<sup>nd</sup> generation has then been realized based on 15 Cr-15 Ni and 15 Cr-25 Ni matrix. The whole tensile and creep program was achieved with test temperatures up to 850°C.

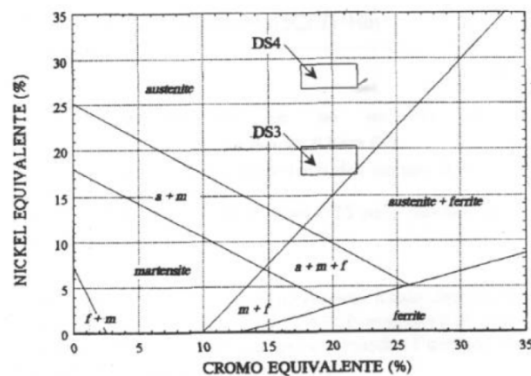


**Fig. 2. Position of the Double-stabilized Steels inside the Shaffler's diagram**

Figure 2 shows the position of the second generation steels inside the Shaffler diagram .

The second generation of DS steels was based on a 15Cr–15Ni matrix, with a complete revision of the chemical composition and on a new matrix 15Cr–25Ni ( DS3 15-15 Ti+Nb, DS4 15-25 Ti+Nb ) [Ref.1]. Two kinds of products were realized in the form of rods (external diameter 8 mm) and cladding pipes (ext. diam. 6,55 mm, internal 5,65). The rods and the pipes were cold-worked with a final section reduction ratio of 20%. The annealing temperature before final cold-working was 1100°C ( 5 minutes in Argon atmosphere ), followed by air cooling.

These 2<sup>nd</sup> generation steels are characterized by a medium grain size, measured by the linear intersection method, in the order of 32-45 micron (N° 7 and 6 ASTM). The optical microscopy showed a low primary precipitation, particularly in the steels with high Nickel content characterized by intergranular dispersion of mixed carbo-nitrides (Ti + Nb). The Vickers hardness values for both the steels varied between 260 (DS4) and 270 kg/mm<sup>2</sup> (DS3) with an applied load of 98 N.

## 2. CREEP BEHAVIOUR

A single lever MAYES jigs with autolevelling arm device has been used to perform creep tests. A three zones P.I.D. controlled furnace and the utilization of S type thermocouples allow the temperature gradient to be maintained at  $\pm 1^\circ\text{C}$  along the gauge length. Test temperatures for DS4 steel range from 550 to 850°C, while DS3 has been tested just up to 750°C. Extensometric device clamped to the specimen's ridges was linked to a pair of capacitance type transducers. The whole system measures elongation of the specimen with an accuracy of 0.2  $\mu\text{m}$ . A completely automatized data logging of strain and elapsed time provide elaboration and drawing of creep curves. The creep tests were performed in constant load conditions.

T (°C)	$\sigma$ (MPa)	$\dot{\epsilon}_m$ (1/h)	t0.2(h)	tR(h)	$\epsilon_f$ (%)	$Z_f$ (%)
550	430	0.258	3291			
	460	0.468	1323	3265	17.23	60.01
	490	0.275	241	1773	11.92	56.84
	580	2953.1	n.m.	0.5	13.59	62.68
650	300	4.796	67.4			
	320	31.676	32.4			
	340	69.051	20.7	213	23.65	66.82
	350	72.149	17.6	137	16.38	65.02
750	110	11.735	119.6	1255	62.52	86.48
	140	12.164	101	492	32.32	84.2
	170	21.593	66	198	37.84	83.02
	200	29.539	31.2	119.5	27.64	80.13

**Table 1. Creep properties of DS3 steel [Ref.1]**

T (°C)	$\sigma$ (MPa)	$\dot{\epsilon}_m$ (1/h)	t0.2(h)	tR(h)	$\epsilon_f$ (%)	$Z_f$ (%)
550	400	0.394	1560	2628	1.56	4.25
	430	0.568	1111	2140	1.67	3.74
	460	1.753	620	1424	2.25	5.97
	490	3.582	125	765	7.79	10.88
	520	6.041	4	575	6.07	18.35
	550	42.436	0.52	238	9.47	26
	580	331.73	0.26	93.4	14.89	44.66
650	250	0.386	2096	10507	16.58	68.76
	300	0.949	18.5	5637	19.34	57.54
	320	2.691	14	2570	12.96	63.2
	340	10.393	3	1067	12.97	54.94
	350	131.188	1.71	126.2	10.68	41.61
	390	572.69	2.02	26	12.52	44.49
	750	90	1.212	1633		
110		1.356	955	3358	36.58	85.11
140		10.312	106	802	28.88	83.34



	170	16.206	34	384	32.29	79.32
	200	64.209	12.8	119	29.19	77.15
	240	356.75	3.5	23.6	19.01	70.75
850	10	0.252	4962			
	40	16.601	112	544	52.69	91.07
	50	17.856	108	354	49.89	90.59
	60	31.42	50.3	167	63.62	92.49
	70	173.07	8.7	46.2	37.35	89.91
	90	285.87	3.4	24.1	44.89	93.08
	110	471.76	6.9	26.1	37.84	86.41

**Table 2. Creep properties of DS4 steel [Ref.1]**

In table 1 and 2, data referring to creep properties of DS3 and DS4 steel respectively, are reported, the meaning of each column being explained as follows:

$\dot{\epsilon}_{m}$  is quantified in  $10^{-6}$  units

$t_{0,2}$  is the time to attain 0.2% of creep elongation

$t_R$  is the rupture-time

$\epsilon_f$  is elongation at failure

$Z_f$  means Reduction of Area at failure

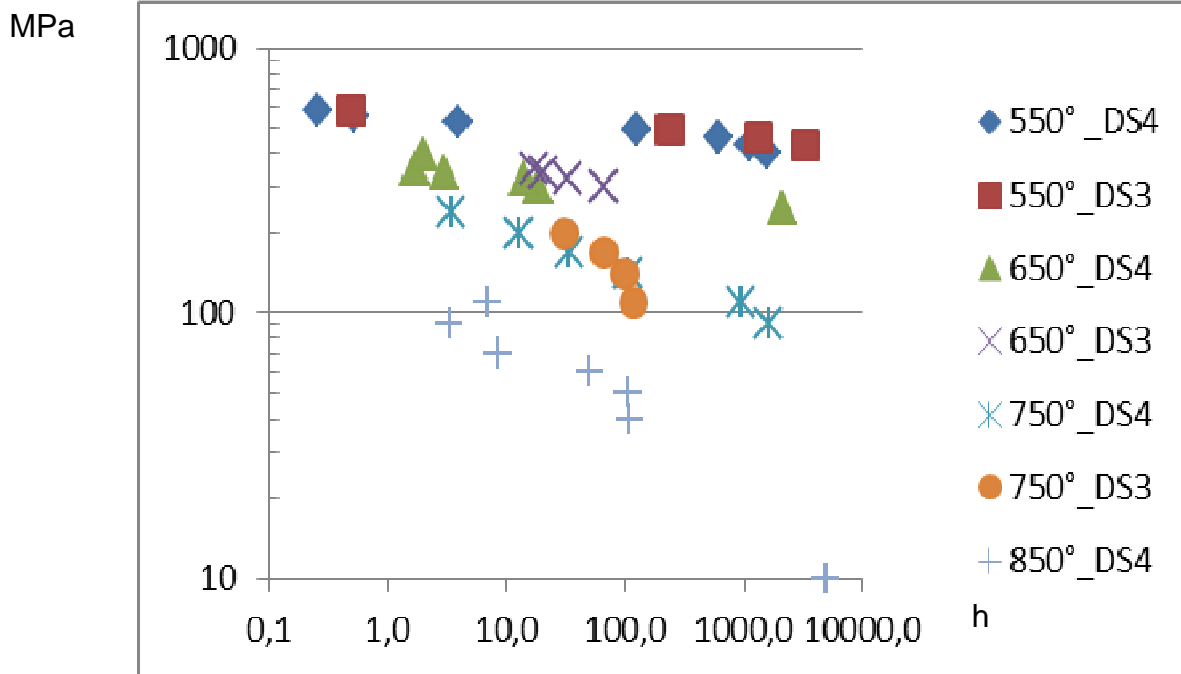


**Fig. 3. Comparison between DS3 and DS4 concerning time to reach a deformation of 0.2%**



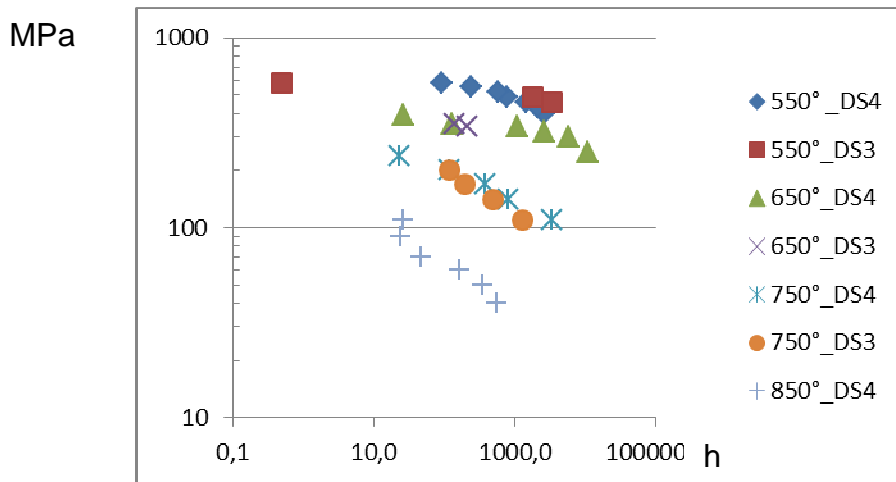


**Fig. 4. Comparison between DS3 and DS4 concerning time to rupture**

In graphs 3 and 4 the times to 0,2% deformation and to rupture are reported. The general trend for these characteristics is very similar to the minimum creep-rate one: DS3 steel seems to behave better than DS4 at stresses lower than about 500 MPa and low temperature (550°C), while for higher temperatures there's a transition point; this better behaviour appears for stresses higher than 340/350 MPa at 650 and about 140 MPa at 750°C. Figure 5 shows a comparison in creep time to rupture between DS3 and other 15Cr-15Ni steels. The double stabilized steel (filled dots) definitely performs a better behavior in comparable temperature conditions.

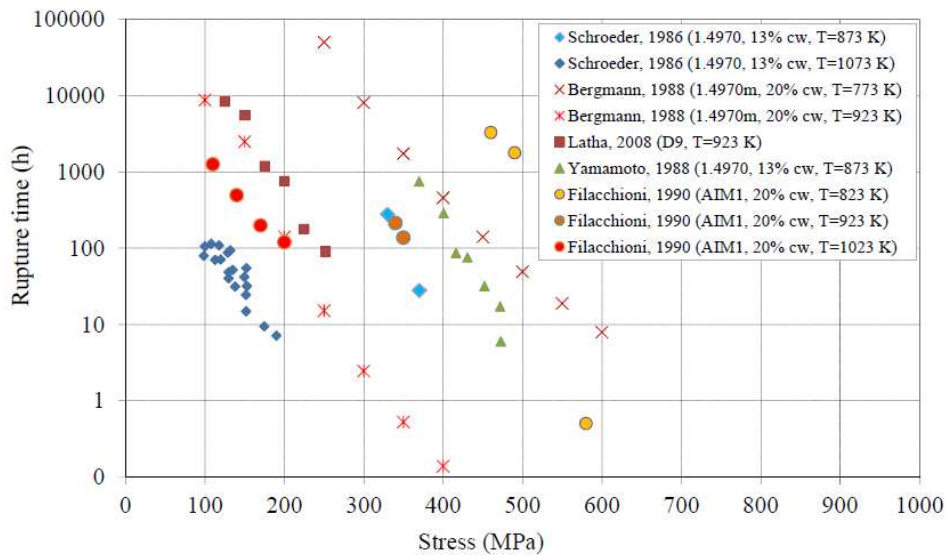


**Fig. 5. Comparison in time to rupture between DS3 (filled dots) and other 15Cr-15Ni steels [Ref. 10]**

### 3. BEHAVIOUR UNDER IRRADIATION; THE RESULTS OF THE EXPERIENCE “SUPERNOVA”

The following graph (figure 6) shows the very promising results obtained in the Supernova experiment in Phénix reactor with an irradiation damage of 89 dpa. One challenge is to find a compromise between low swelling and good ductility after irradiation. The comparison of advanced austenitic steels shows the beneficial effect of cold working, increasing Ni percentage, stabilization by Ti and Nb addition performed on the second generation stainless steels. The comparison between micrographies shows how the Limited swelling of advanced austenitic steels is consistent with low amount of cavities (figure 7).

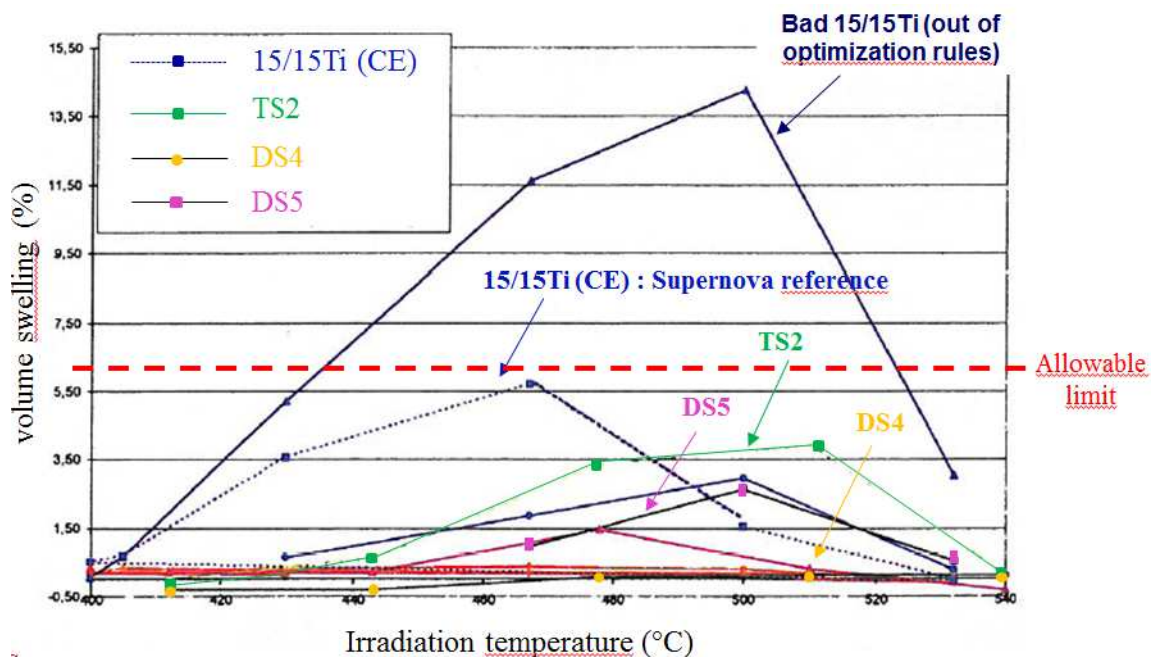


Fig. 6. Limited swelling of the advanced austenitic steels [Ref. 11]

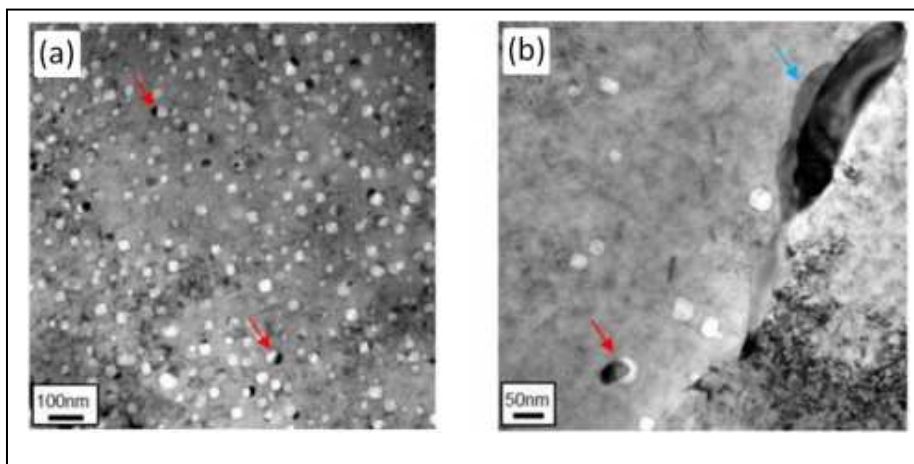


Fig. 7. Low amount of cavities in the advanced austenitic stainless steel (b) if compared to the non-optimized 15-15 Ti (a) [Ref. 11]

## 4. PRELIMINARY RESULTS OF THE CORROSION TESTS PERFORMED AT ENEA BRASIMONE

The preliminary results presented in the following pages refer to corrosion tests performed in ENEA Brasimone laboratories between June and August 2013. The boundary conditions are listed below:

- Specimen considered: DS3 (15Cr-15Ni) DS4 (15Cr-25Ni) and DS5 (15Cr-25Ni)
- Stagnant lead environment: the specimen is plunged for half of its length in an Al<sub>2</sub>O<sub>3</sub> glass filled with molten lead;
- Oxidizing atmosphere: oxygen content approximately between 10<sup>-6</sup> and 5.10<sup>-4</sup> wt%
- Temperature of the bath kept at 550°C
- Duration of the test: 900h (DS4)-1000h (DS3,DS5)

The micrographies show that the sample has undergone oxidizing processes both in the plunged side and in the not submerged one; the thickness of the oxide layer is narrower in the not plunged side (see fig. 8).

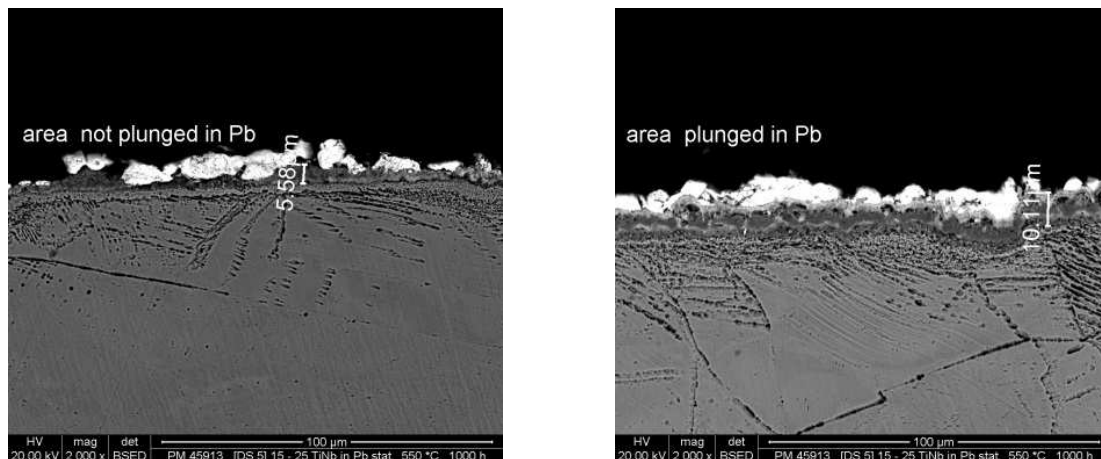


**Fig.8. Difference in oxide width between the plunged and the not plunged side of the sample in DS5 steel**

The oxide layer thickness ranges around an average width of 8-10 μm in the plunged area for the steels with higher content in Nb ( DS3 and DS5). Concerning the steel with lower content in Nb (the DS4), instead, the oxide layer thickness ranges around an average width of 15-20 μm (fig. 9). Concerning the expected width of the oxide layer for an austenitic steel, our results don't seem to be in agreement with the ones obtained in other experimental campaigns in LBE (see fig 10). In two of the DS steels, the DS3 and the DS5, the ones with the higher content in Nb, the oxide width appears a few microns larger than the 5-6 microns expected after 1000 h of exposure. In the DS4 this value results even doubled.

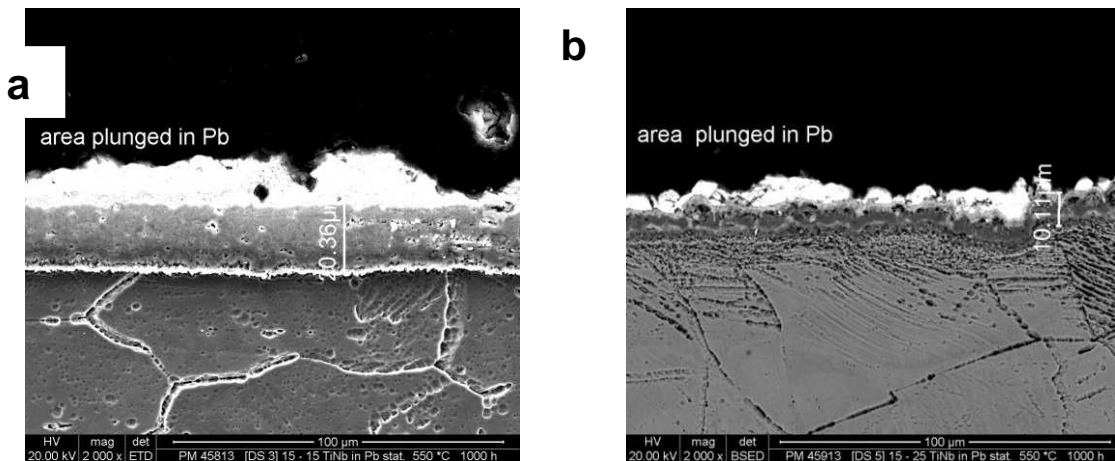


**Fig.9.** Comparison between the width of the oxide layer formed in the DS4 (15Cr-25Ni, low Nb) (a) and in the DS5 (15Cr-25Ni, high Nb) (b)

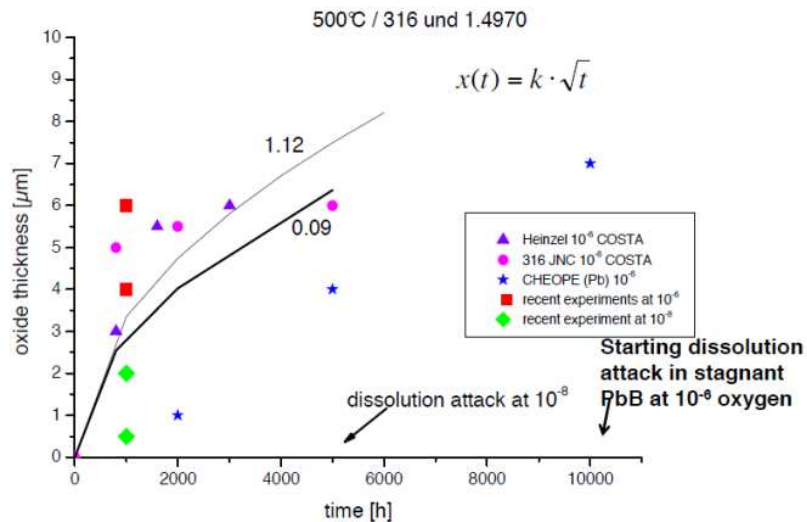


**Fig.10.** Thicknesses of oxide [Ref.14] as a function of corrosion duration for austenitic steels in LBE for 500°C temperature range

In the plunged side, where lead comes in contact with the austenitic matrix, a transition zone, with probable migration of Cr and Ni, has been detected in each one of the 3 steels (see fig. 11). This ferritic zone between the external oxide layer and the inner austenitic substrate isn't detectable in the not plunged side of the specimen. The average dimension of the ferritic zone of transition is 5-7 μm. Concerning DS3 and DS5, the dimension of the whole area affected by oxidation processes, resulting by the sum of the oxide layer and the ferritic zone, presents an average value of about 10 μm but it reaches a maximum width of about 30 μm in the lower part of the crucible (see fig. 12).

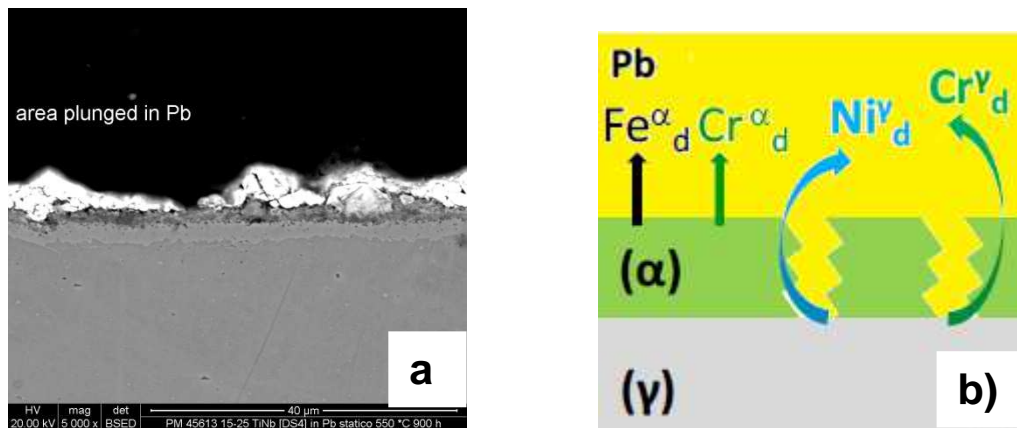


**Fig. 11.** Transition zone (faded grey) only detectable in the plunged side of the sample (a) and schematic drawing of the formation of the ferritic zone of transition in an austenitic steel (b)

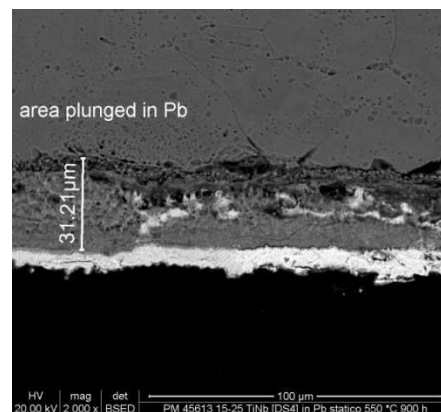


**Fig.12.** Maximum width of oxide layer and transition zone together

The observations reported in this paper must be considered just as a first step towards the characterization in lead of these steels; more precise informations will come out in the future as soon as new material, deriving from the procurement described in this report, will be available.

## 5. Scope of the Supply

The aim of the present Supply is

- the implementation and reporting concerning the manufacturing process for the production of DS4 stainless steel plates;
- the delivery of ingots and the production of DS4 SS plates, (about 50 kg)
- the preliminary characterization by tensile tests
- the shipment of the plates by the C.R. ENEA Brasimone, Italy.

## 6. Technical Specification – DS4 Steel

### *Chemical Composition*


#### **Weight Percent**

C	desiderata 0,05	specifica	0,04<C<0,06
Cr	desiderata 15	specifica	14<Cr<16
Ni	desiderata 25	specifica	24,5<Ni<25,5
Mo	desiderata 1,5	specifica	1,2<Mo<1,8
Mn	desiderata 1,5	specifica	1,2<Mn<1,8
Si	desiderata 0,9	specifica	0,8<Si<1
Ti	desiderata 0,15	specifica	0,1<Ti<0,3
Nb	desiderata 0,15	specifica	0,1<Nb<0,3
V		specifica	V<300 ppm
N	desiderata 150 ppm	specifica	N<200 ppm
P	desiderata 400 ppm	specifica	350ppm<P<450ppm
B	desiderata 50 ppm	specifica	B<60 ppm
Al	desiderata 150 ppm	specifica	Al < 200ppm
S	desiderata 70 ppm	specifica	S<150ppm
Cu		specifica	Cu<0,1 ppm
Co		specifica	Co<0,1 ppm
Ca		specifica	Ca<0,03 ppm
Ta		specifica	Ta<0,03 ppm
Zr		specifica	Zr<0,03 ppm
W		specifica	W<0,03 ppm

### ***Production***

- Melting and re-melting in void (VIM process)
- Production of the lab ingots



 <b>Ricerca Sistema Elettrico</b>	<b>Sigla di identificazione</b>	<b>Rev.</b>	<b>Distrib.</b>	<b>Pag.</b>	<b>di</b>
	ADPFISS – LP2 – 067	0	L	13	17

- Homogenization Annealing 1200°C per 2 ore
- Chemical and metallographic analysis.
- Production of the plates by hot rolling; final thickness suitable to reach 15 mm thickness after CW
  - Max heating temperature: 1150°C
  - Min rolling temperature: 800°C
- Ultrasound and RX check to discard the defective parts
- Final Annealing before CW: 1100°C for 5 minutes, subsequent cooling in Argon atmosphere
- Cold Working; section reduction ratio 20% with final thickness 15 mm
- Chemical and metallographic analysis.

### ***Characterization Tests***

- 10 tensile tests at room temperature according to the ASTM E8 rules (constant elongation rate);
- 10 tensile tests at 550°C according to the ASTM E21 rules (constant elongation rate);

### ***Documentation follow up***


The supply will be completed by a documentation set follow up. The following documents will be delivered:

- Report on the manufacturing of DS4 SS plates ([Annex 1](#));
- Composition check for each ingots and plates produced ([Annex 2](#));

## **7. BIBLIOGRAPHY**

- [1] G.FILACCHIONI, A.CALZA BINI and L.PILLONI: Development of a New Family of Austenitic Alloys: The Double Stabilized Stainless Steels. Design Criteria and Metallurgical Properties - Proceedings of Int Conf. on Evolution of Advanced Materials, Milan (1989), 89-94



 <b>Ricerca Sistema Elettrico</b>	<b>Sigla di identificazione</b>	<b>Rev.</b>	<b>Distrib.</b>	<b>Pag.</b>	<b>di</b>
	ADPFISS – LP2 – 067	0	L	14	17

## ANNEX – 1 - Fabbricazione lingotto DS4

Il lingotto DS4 (fig.1) è stato realizzato all'interno del laboratorio "Tecnologie Fusorie & Chimica Metallurgica", mediante la tecnologia fusoria in vuoto VIM (Vacuum Induction Melting), che è il processo di fusione più versatile per la produzione di quasi tutte le leghe speciali base Fe, Ni e Co.

L'impianto VIM del CSM (ALD-Vacuum Technologies) (fig. 2 ) impiegato per la produzione dei lingotti, possiede le seguenti caratteristiche tecniche:

- Intervalli di fusione: 1300 – 1600 °C;
- Atmosfera: Vuoto/gas inerte;
- Pressione di lavoro: da  $5 \times 10^{-5}$  mbar a 300 mbar;
- Range di misura temperature: da 750 a 1800°C (tramite termocoppie e pirometri ottici);
- Colaggio: Lingottiera/Guscio ceramico;
- Volume di fusione/colaggio: da 1 a 11 dm<sup>3</sup>;




**Fig. 1 – Lingotto DS4**

Il processo di fusione della carica avviene tramite una bobina di rame, raffreddata ad acqua, attraverso la quale passa una corrente alternata che avvolge il crogiolo di refrattario generando così delle correnti parassite nel materiale di carica che si scalda per effetto joule.

L'agitazione ('stirring magnetico') che il processo genera nel bagno garantisce sia la omogeneizzazione e il controllo più accurato della chimica e della temperatura del fuso, sia il trasporto di materia necessario per lo svolgimento delle reazioni chimico-fisiche richieste, come per esempio, il degasaggio.

Tale processo garantisce inoltre un'esatta composizione e riproducibilità del prodotto. Il ciclo di fusorio in un forno VIM è strutturato in diversi passaggi: carica, fusione, affinazione, analisi chimica e correzione della composizione, colaggio.

Il materiale di carica è comprensivo degli elementi leganti, eccetto i costituenti reattivi, che vengono introdotti successivamente mediante un sistema di carica posto

 <b>Ricerca Sistema Elettrico</b>	<b>Sigla di identificazione</b>	<b>Rev.</b>	<b>Distrib.</b>	<b>Pag.</b>	<b>di</b>
	ADPFISS – LP2 – 067	0	L	15	17

sulla sommità del forno. Durante la fusione e l' affinazione avvengono reazioni quali il degasaggio e la disossidazione.

Alla fine del periodo di affinazione vengono introdotti, se necessari, gli elementi reattivi quali Si e Mn.



**Fig. 2 – Impianto VIM (ALD-Vacuum Technologies) presso il CSM**

Dopo un tempo richiesto per il mescolamento ottimale del bagno si procede ad un'analisi chimica ed ad eventuali aggiunte di alliganti nel caso di carenze nella composizione. Alla fine il fuso viene colato in lingottiera.

In questo caso per i materiali di carica sono state utilizzate materie prime con purezza non inferiore al 99.9%.

Sono stati prodotti n°1 lingotto, di dimensioni 200x100 mm e altezza 400mm per un totale di circa 40kg di materiale.

Il ciclo fusorio seguito è mostrato inoltre in fig. 3. Il grafico riporta l'andamento dei valori di vuoto, di potenza e di temperatura del forno ad induzione in funzione delle diverse fasi del processo.

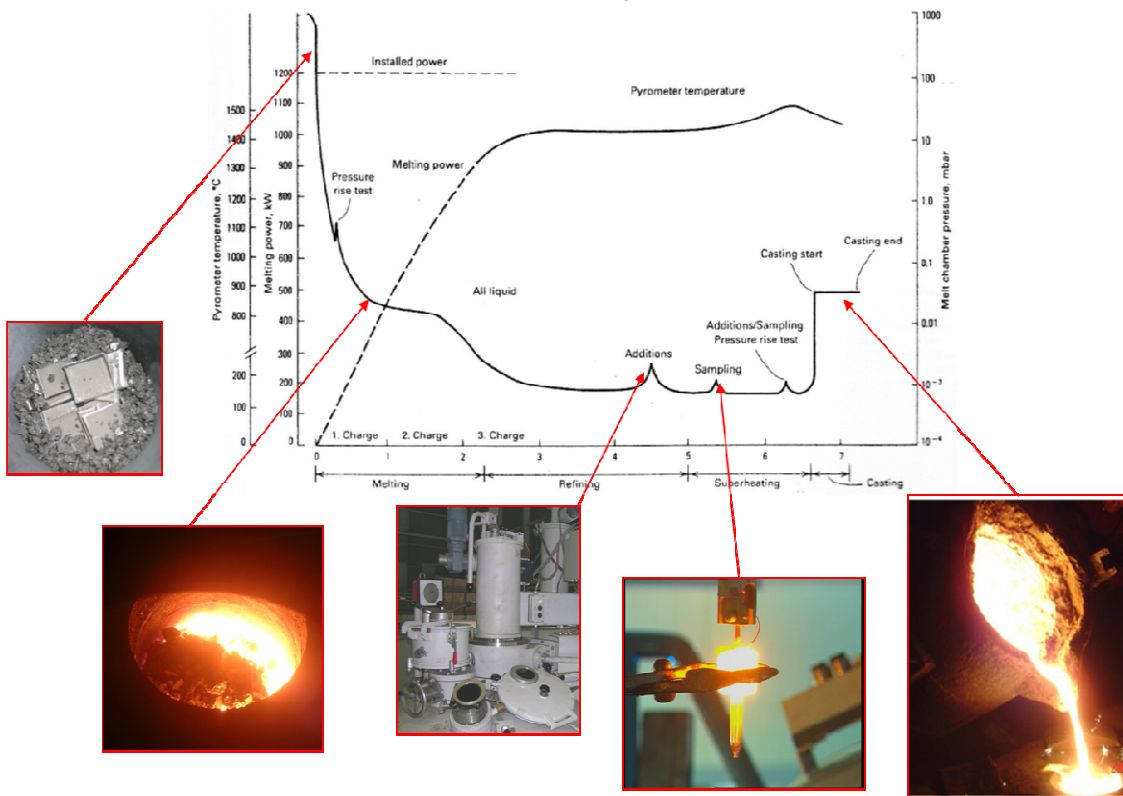


Fig. 3 - Differenti fasi del ciclo fusorio

I risultati ottenuti in termini di composizione chimica sono riportati nella tabella di seguito, in cui si evince il perfetto raggiungimento dei target composizionali richiesti.

Rapporto d'analisi N. 8392      Data di richiesta : 2014-07-15

-0195-VM 2882

SIGLA CAMP.	BAL. Fe	% C	% S	% N	% P	% Mo	% Co	% Cr	% Si	% Ti
-0195-	BAL	0.041	0.0082	0.013	0.037	1.46	<0.01	14.8	0.88	0.17
MINIMO	BAL	0.0400	0	0	0.0350	1.20	0	14.0	0.80	0.100
MAXIMO	BAL	0.060	<0.015	<0.02	0.0450	1.80	<0.1	16.0	1.00	0.300

SIGLA CAMP.	% Mn	% Cu	% Nb	% B	% Al	% Zr	% W	% Ca	% Ta	% Ni
-0195-	1.48	0.06	0.20		0.013		<0.05			24.6
MINIMO	1.20	0	0.100	0	0	0	0	0	0	24.5
MAXIMO	1.80	<0.1	0.300	0	0.015	0.03	0.03	0.03	0.03	25.5

ESEGUITO DA : /MARCHESINI/PACIELLO

Responsabile di laboratorio  
Firma: *[Signature]*

Specifica richiesta

Fig. 4 – composizioni chimiche lega madre

## ANNEX – 2 – Rapporto d'Analisi Lingotto

8352 DOCUMENTO PER USO INTERNO

RICHIEDENTE:SORCI

COMMESSA:RD010132

Rapporto d'analisi N. 8352

Data di richiesta : 2014-07-15

-0195-VM 2882

SIGLA CAMP.	BAL Fe	% C	% S	% N	% P	% Mo	% Co	% Cr	% Si	% Ti
-0195-	BAL	0.041	0.0082	0.013	0.037	1.46	<0.01	14.8	0.88	0.17
MINIMO	BAL	0.0400	0	0	0.0350	1.20	0	14.0	0.80	0.100
MAXIMO	BAL	0.060	<0.015	<0.02	0.0450	1.80	<0.1	16.0	1.00	0.300

SIGLA CAMP.	% Mn	% Cu	% Nb	% B	% Al	% Zr	% W	% Ca	% Ta	% Ni
-0195-	1.48	0.06	0.20		0.013		<0.05			24.6
MINIMO	1.20	0	0.100	0	0	0	0	0	0	24.5
MAXIMO	1.80	<0.1	0.300	0	0.015	0.03	0.03	0.03	0.03	25.5

ESEGUITO DA : /MARCHESINI/PACIELLO

Responsabile di laboratorio

Firma 